Silver Chemistry Hot Paper

How to cite: *Angew. Chem. Int. Ed.* **2020**, *59*, 19910–19913
International Edition: doi.org/10.1002/anie.202008874
German Edition: doi.org/10.1002/ange.202008874

Idiosyncratic $Ag_7Pt_2O_7$: An Electron Imprecise yet Diamagnetic Small Band Gap Oxide

*Gohil S. Thakur, Robert Dinnebier, Thomas C. Hansen, Wilfried Assenmacher, Claudia Felser, and Martin Jansen**

Dedicated to Professor Herbert Roesky on the occasion of his 85th birthday

Abstract: *The seminal qualitative concepts of chemical bonding, as presented by Walter Kossel and Gilbert Newton Lewis back in 1916, have lasting general validity. These basic rules of chemical valence still serve as a touchstone for validating the plausibility of composition and constitution of a given chemical compound. We report on $Ag_7Pt_2O_7$, with a composition that violates the basic rules of chemical valence and an exotic crystal structure. The first coordination sphere of platinum is characteristic of tetravalent platinum. Thus, the electron count corresponds to $Ag_7Pt_2O_7{*}e^-$, where excess electrons are associated with the silver substructure. Such conditions given, it is commonly assumed that the excess electrons are either itinerant or localized in Ag–Ag bonds. However, the material does not show metallic conductivity, nor does the structure feature Ag-Ag pairs. Instead, the excess electrons organize themselves in 2e–4c bonds within the silver substructure. This subvalent silver oxide reveals a new general facet pertinent to silver chemistry.*

The chemistry of silver, dominated by the oxidation state of +1, appeared to be essentially settled, and some recent realizations of the higher oxidation states +2 and +3, for example, in extended fluorides and oxides,[1,2] did not come as a surprise, in view of similar behaviors of the group homologues. However, more recently, some singular observations started to consolidate. Unusually short silver-silver separations in oxides with high silver contents have turned out not to be an exception, but a general aspect of the chemistry of monovalent silver.[3] In such silver-rich oxides, silver atoms, although positively charged, tend to flock together forming partial structures that are topologically reminiscent of elemental silver, lending support to assumingly attractive unconventional d^{10}-d^{10} interactions between silver atoms.[3b] Another comparable situation seems to emerge now.

Some individual ternary silver oxides, exhibiting odd compositions, and accommodating excess valence electrons have been communicated.[4] Here we report on constitutionally well-confirmed new $Ag_7Pt_2O_7$ which is not electron-precise either and constitutes a particularly illustrative example for such a case of subvalence. Since the first coordination sphere of platinum perfectly meets the geometry as commonly found for Pt^{4+}, the excess electrons have to be accommodated by the silver substructure. However, neither metallic behavior, as were to be expected if the excess electrons are itinerant, nor any structural indication for the presence of homo-atomic 2*e*-2*c* bonds has been revealed. Moreover, corresponding to the odd number of electrons per unit cell, such material should show a paramagnetic response which is not found experimentally.

Shiny black $Ag_7Pt_2O_7$ samples were synthesized as a polycrystalline material by heating appropriate mixtures of Ag_2O and PtO_2 under gently elevated oxygen pressure. The compound is insensitive to humid air and decomposes in three steps, starting at 410 K with a loss of a small amount of oxygen ($\approx$0.33 mol), followed by another partial loss ($\approx$0.33 mol) starting at 580 K, and is fully reduced to a mixture of elemental Ag and Pt upon heating above 875 K (Supporting Information, Figure S2).

Since all efforts made to grow single crystals of a size suited for single-crystal X-ray diffraction failed (the samples morphology is displayed in Figure S3), we had to resort to X-ray and neutron powder diffraction techniques for crystal structure determination and refinement. The profiles obtained from a combined X-ray and neutron powder profile refinement are shown in Figure 1.

Since the structure model obtained is quite complex (Figure 1), we regarded it as essential to corroborate the indexing and space group symmetry assumed during crystal

[*] Dr. G. S. Thakur, Prof. Dr. C. Felser, Prof. Dr. M. Jansen
Max-Planck-Institut für Chemische Physik fester Stoffe
Nöthnitzer Str. 40, 01187 Dresden (Germany)
E-mail: M.Jansen@fkf.mpg.de
Prof. Dr. R. Dinnebier, Prof. Dr. M. Jansen
Max-Planck-Institut für Festkörperforschung
Heisenbergstr. 1, 70569 Stuttgart (Germany)
Dr. T. C. Hansen
Institut Laue-Langevin
71 avenue des Martyrs, 38000 Grenoble (France)
Dr. W. Assenmacher
Institut für Anorganische Chemie
Rheinische-Friedrich-Wilhelms Universität
Römerstr. 154, 53117 Bonn (Germany)
Supporting information and the ORCID identification number(s) for the author(s) of this article can be found under: https://doi.org/10.1002/anie.202008874.

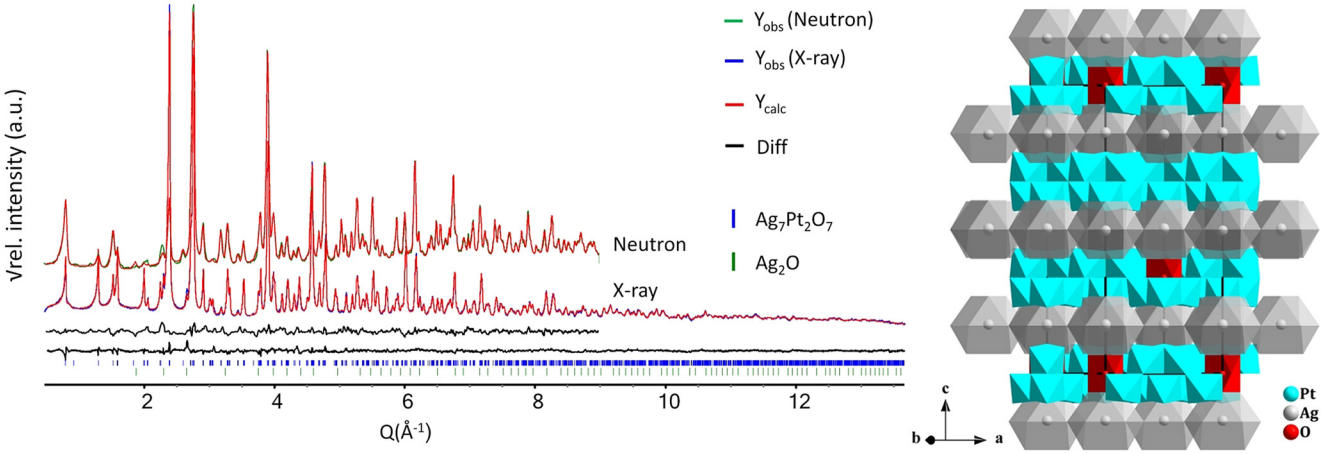

Figure 1. Left) Scattered X-ray (blue line) and neutron diffraction intensities (green line) of $Ag_7Pt_2O_7$ at ambient conditions as a function of Q ($=4\pi \sin(\theta)/\lambda$); the best-combined Rietveld fit profiles (red lines) and the difference curves between the observed and the calculated profiles (gray lines) are shown. The square root of the intensity is displayed for better visibility of smaller reflections. Vertical bars represent the allowed Bragg's reflection for the two phases. Right) Crystal structure of $Ag_7Pt_2O_7$.

structure determination from powder data by electron diffraction on individual crystallites. As shown in Figures S4 and S5, the single-crystal diffraction patterns unambiguously confirm the diffraction symbol as extracted from powder data. Finally, the composition of $Ag_7Pt_2O_7$ as obtained from crystal structure analysis was verified by ICP-OES and SEM-EDS analyses (Supporting Information, Table S1).

$Ag_7Pt_2O_7$ displays a novel structure with several interesting structural features which are unprecedented. The unique crystal structure is best described starting with the arrangement of the metal atoms, which, for platinum and silver in total, follows the motif of a cubic closed packing (*ccp*), with 9 layers of 9×9 grids of 2D close-packed meshes constituting the content of the unit cell (Figures 2a,b). The layers at $z=$ 1/6, 1/2 and 5/6 are composed of silver alone. All the oxygen atoms occupy octahedral voids of the *ccp* arrangement of metals, though significantly off-center. Each layer of octahedral voids is filled to a ratio of 7/9. For platinum a quite regular octahedral coordination results, where the average Pt–O bond length of 2.04 Å is indicative of the +4 oxidation state for platinum in 6-fold coordination.[5] The PtO_6 primary building units are condensed by sharing common edges, three forming a triangular secondary cluster, while each of the latter is connected to three other of the same kind on a second level (Figures 2c,d). The tertiary structure of the resulting 2D polyanion thus corresponds to a humped slab (Figure 2c). While most of the silver atoms are under-coordinated, Ag(5) is coordinated octahedrally by oxygen atoms at the right distances. The structural function of Ag(5) is twofold, it is linking each two of the 2D $[Pt_2O_7]^{6-}$ slabs by connecting respective top and bottom triangular faces (Figure 2d), and it is completing the 2D dense-packed layers of silver atoms at $z=1/6$, 1/2 and 5/6 (Figure 3a). The remaining silver atoms accumulate in the shape of approximate cuboctahedra, each centered by a silver atom and connected via edges to three symmetry equivalents forming a honeycomb pattern (Figure 3a).

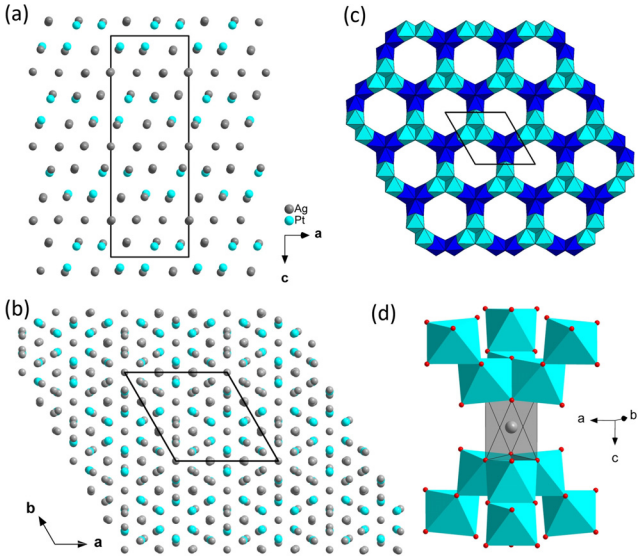

Figure 2. Different aspects of the $Ag_7Pt_2O_7$ structure. a,b) Cubic close-packed array of Ag and Pt atoms, views along *b* and *c* directions, respectively. c) 2D $(Pt_2O_7)_n^{6n-}$ polyoxoanion slab (octahedra in cyan on the upper level; the lower level is depicted in dark blue). d) Link between Pt_2O_7 slabs mediated by Ag(5); the resulting AgO_6 octahedron is indicated by gray faces.

Notably, the relevant silver-silver separations are short, ranging from 2.86 Å (Ag(3)-Ag(4)) to 3.10 Å (Ag(3)-Ag(3)). The shortest distance of 2.86 Å is certainly smaller than the Ag-Ag separations in elemental silver (2.89 Å), but somewhat larger than those observed in other subvalent silver compounds.[4,6] Three square faces of the Ag_{13}-cuboctahedra are capped by oxygen atom O(5) at a distance of 2.26 and 2.36 Å (for Ag3-O5 and Ag4-O5, respectively), this oxygen atom, in turn, forms one of the vertices of the adjoining PtO_6 octahedra. Each of the cuboctahedra from adjacent layers is interconnected by means of O(3), establishing a dumbbell like motif (Figure 3b).

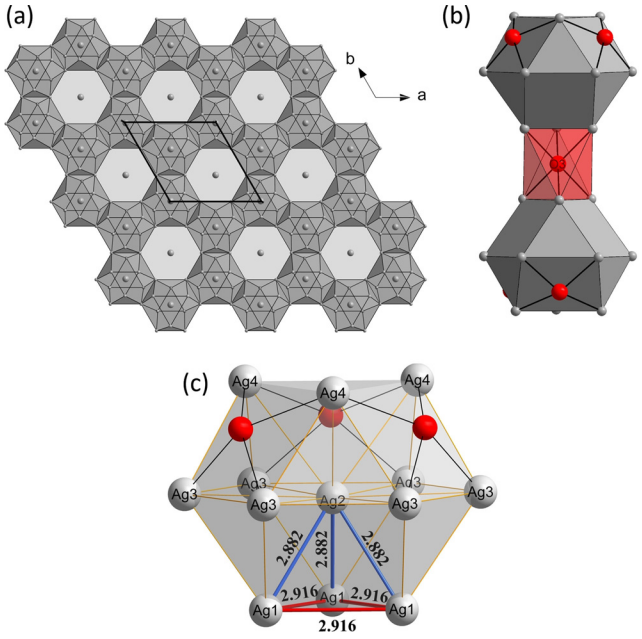

Figure 3. Aspects of the silver substructure. a) Single 2D honeycomb-like layer of interconnected cuboctahedral Ag_{13} clusters with Ag(5) completing the middle 2D close-packed layer, b) Ag_{13} clusters from adjacent layers interlinked by O(3), c) an individual Ag_{13} cluster (distances in Å).

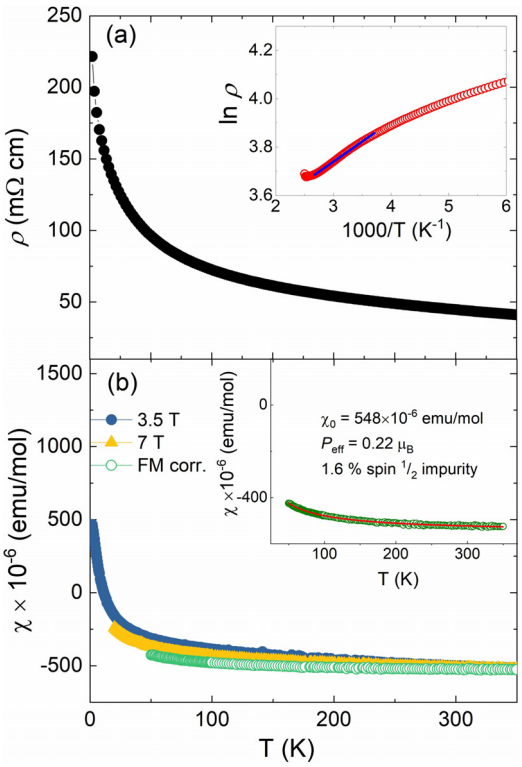

Figure 4. a) Resistivity plots for a sintered pellet of $Ag_7Pt_2O_7$ showing semiconducting-like behavior. Inset: Arrhenius plot of resistivity with a linear fit (blue) in the high-temperature region (280–350 K). b) Susceptibility of $Ag_7Pt_2O_7$ at different applied magnetic fields. Inset: Curie fit (red line).

Resistivity measurements performed on a sintered pellet revealed semiconducting behavior of the compound with an approximate band gap of 300 meV (Figure 4a), while the magnetic susceptibility as a function of temperature clearly reflects diamagnetic response (Figure 4b). A fit to the experimental susceptibility data, corrected for a slight ferromagnetic impurity, using a sum of temperature independent diamagnetic and Curie terms according to $\chi = \chi_0 + \frac{C}{T}$ is shown in the inset of Figure 4b. The fitted Curie constant $C = 5.6 \times 10^{-3}\,cm^3\,mol^{-1}\,K$ corresponds to about 1.6% of localized $S = {}^1/_2$ impurity centers.

The composition as obtained from crystal structure determination and chemical analyses is suggesting an electron count conforming to the formula $(Ag^+)_7(Pt^{4+})_2(O^{2-})_7 * 1e^-$, which is obviously in conflict with the physical properties as recorded. Resistivity in the range of 50 mΩ cm at 300 K and its temperature dependence exclude the presence of itinerant electrons, on the other hand, an odd number of localized electrons per unit cell should result in a paramagnetic response, which was not observed experimentally.

In order to resolve the conflict between the electron count based on the crystal structure and physical properties, we examined the structure model for particular contractions of interatomic Ag-Ag distances, which might be indicative of localizations of the excess electrons. Indeed, such regions can be identified within the cuboctahedral cluster units. While the upper half of the Ag_{13} unit displayed in Figure 3c is capped by oxygen atoms at binding distances, the bottom features apparently unforced contractions of Ag-Ag separations within a group of four silver atoms forming an approximately tetrahedral, strictly speaking a trigonal pyramidal, arrangement. Three out of the six Ag-Ag distances, the edges of the approximate tetrahedron, are shorter (2.882 A) than those in elemental silver, three are slightly longer (2.916 A) and are connected to oxygen atom O3. These voids are the most probable sites accommodating the excess electrons. The electrons must localize pairwise, in order to comply with the diamagnetic response of the bulk material. However, per unit cell, there are six such sites, but only nine excess electrons. These implications may be settled in two ways, either the electron pairs localize within part of the Ag_4 aggregates in a non-periodic fashion or by establishing long-range order, where the latter would imply a superstructure to develop. Since the structural differences between occupied and empty Ag_4 voids will be small, proving the existence of a respective supercell constitutes a particular challenge. For this purpose, additional high-resolution neutron diffraction data were collected with enhanced counting statistics. Indeed, beyond the Bragg reflections of the main phase $Ag_7Pt_2O_7$ and of traces of Ag_2O, these data include tiny intensity features that can be indexed together with the subcell reflections assuming a commensurate modulation with a propagation vector of ${}^1/_2\ {}^1/_2\ 0$. Unfortunately, the resulting unit cell is of a size that does admit neither a detailed refinement of the atomic parameters nor computational analyses of the electron localization. Figure S6 displays a comparison of the neutron diffraction profile fits for the subcell and the $p = {}^1/_2,\ {}^1/_2,\ 0$ super-cell, providing evidence for experimental intensities not

matched by the subcell and the minor impurity phases present. This finding is getting support by a Pawley fit (Figure S7). The picture obtained would reconcile all observations made.

The title compound thus represents a rather unconventional oxide, with respect to crystal structure, properties, and bonding scheme. Conventional chemical bonding is constituting the prevailing share of lattice energy, while superimposed attractive $5d^{10}$–$5d^{10}$ bonding interactions[3b] and excess electrons occupying bonding 4*s* and 4*p* states interact in a synergetic fashion resulting in local clustering of silver atoms, embedded in an extended solid oxide matrix. This new bonding pattern seems to be gaining general validity by analogous cases reported. In Ag_5SiO_4,[4d] and isostructural Ag_5GeO_4,[4b,c] octahedral silver clusters are hosting an electron pair in the lowest energy skeleton MO, while in $Ag_{16}B_4O_{10}$ trigonal pyramidal voids formed by silver atoms accommodate electron pairs.[7] In all latter examples, the number of contracted sites and of electron pairs to be accommodated correspond such that no structural implications as encountered for the title compound are resulting. In particular, the very recent findings for $Ag_{16}B_4O_{10}$, featuring the same umbrella-like Ag_4 entities[7] are lending support to the interpretation presented here for $Ag_7Pt_2O_7$.

To summarize, we report on a new silver subvalent ternary oxide, $Ag_7Pt_2O_7$, displaying an exotic novel crystal and electronic structure. At first glance, the electron count based on the crystal structure appeared to be in conflict with its bulk semiconducting and diamagnetic properties. This seeming inconsistency has been resolved by proving the presence of pairwise localization of the excess electrons in the centers of Ag_4 clusters embedded in the extended oxide structure. The novel bonding motif is reminiscent of electrides or charge density waves in solid materials. However, there appears to be a closer analogy to the "Polyhedral Skeletal Electron Pair Theory" as originally developed by Wade and Mingos for molecular cluster chemistry.[8] In this sense the excess electron pair would occupy the lowest bonding skeleton MO of the embedded silver clusters (irreducible representation a_1 for T_d, or C_{3v}, which is the correct point group within the limits of experimental error).

Acknowledgements

The authors thanks Walter Schnelle and Ralf Koban for susceptibility and resistivity measurements. Open access funding enabled and organized by Projekt DEAL.

Conflict of interest

The authors declare no conflict of interest.

Keywords: electron diffraction · silver clusters · silver oxoplatinate · subvalent silver

[1] B. G. Müller, *Angew. Chem. Int. Ed. Engl.* **1987**, *26*, 1081; *Angew. Chem.* **1987**, *99*, 1120.
[2] a) B. Standke, M. Jansen, *Angew. Chem. Int. Ed. Engl.* **1985**, *24*, 118; *Angew. Chem.* **1985**, *97*, 114; b) B. Standke, M. Jansen, *Angew. Chem. Int. Ed. Engl.* **1986**, *25*, 77; *Angew. Chem.* **1986**, *98*, 78; c) P. Fischer, M. Jansen, *Acta Chem. Scand.* **1991**, *45*, 816.
[3] a) M. Jansen, *J. Less-Common Met.* **1980**, *76*, 285; b) M. Jansen, *Angew. Chem. Int. Ed. Engl.* **1987**, *26*, 1098; *Angew. Chem.* **1987**, *99*, 1136; c) H. Schmidbaur, A. Schier, *Angew. Chem. Int. Ed.* **2015**, *54*, 746; *Angew. Chem.* **2015**, *127*, 756.
[4] a) W. Beesk, P. G. Jones, H. Rumpel, E. Schwarzmann, G. M. Sheldrick, *J. Chem. Soc. Chem. Commun.* **1981**, 644; b) M. Jansen, C. Linke, *Angew. Chem. Int. Ed. Engl.* **1992**, *31*, 653; *Angew. Chem.* **1992**, *104*, 618; c) M. Jansen, C. Linke, *Z. Anorg. Allg. Chem.* **1992**, *616*, 95; d) C. Linke, M. Jansen, *Inorg. Chem.* **1994**, *33*, 2614; e) M. Schreyer, M. Jansen, *Angew. Chem. Int. Ed.* **2002**, *41*, 643; *Angew. Chem.* **2002**, *114*, 665.
[5] a) J. Hauck, *Z. Naturforsch.* **1976**, *31b*, 1179; b) G. S. Thakur, H. Reuter, C. Felser, M. Jansen, *Z. Naturforsch.* **2019**, *73b*, 831; c) G. S. Thakur, H. Reuter, H. Rosner, G. H. Fecher, C. Felser, M. Jansen, *Dalton Trans.* **2019**, *48*, 5058; d) R. D. Shannon, C. T. Prewitt, *Acta Crystallogr. Sect. B* **1969**, *25*, 925.
[6] a) S. Ahlert, W. Klein, O. Jepsen, O. Gunnarsson, O. Krogh Andersen, M. Jansen, *Angew. Chem. Int. Ed.* **2003**, *42*, 4322; *Angew. Chem.* **2003**, *115*, 4458; b) M. Jansen, M. Bortz, K. Heidebrecht, *J. Less-Common Met.* **1990**, *161*, 17.
[7] A. Kovalevskiy, C. Yin, J. Nuss, U. Wedig, M. Jansen, *Chem. Sci.* **2020**, *11*, 962.
[8] a) K. Wade, *Adv. Inorg. Chem. Radiochem.* **1976**, *18*, 1; b) D. M. P. Mingos, *Acc. Chem. Res.* **1984**, *17*, 311.

Manuscript received: June 25, 2020
Revised manuscript received: July 22, 2020
Accepted manuscript online: July 28, 2020
Version of record online: September 15, 2020

